COMPLEX WAVELET PACKETS FOR MULTICARRIER MODULATION

Tushar K. Adhikary and Vellenki U. Reddy

Department of Electrical Communication Engineering
Indian Institute of Science, Bangalore-560012, India

ABSTRACT

In this paper, we first discuss two approaches for designing complex wavelet packets which can be used as orthogonal carriers for modulations like QAM and PM, and then compare the performance of the wavelet packet based modulation scheme with that of discrete multitone modulation using DFT bases. The results show that the wavelet packet based scheme yields lower average bit error probability compared to the DFT based scheme. The improved performance of the wavelet packet based scheme is because of the spectrally contained nature of the wavelet packet bases which are under the control of the designer.

1. INTRODUCTION

In multicarrier modulation, the channel is partitioned into a number of subchannels, each with its own associated basis. Discrete multitone modulation (DMT) uses DFT bases, which exhibit desired orthogonality. However, for these bases, the stopband attenuation is very poor and overlap of subchannels is high thereby resulting in poor performance for the channels that introduce distortion.

Any complex multicarrier bases, to be used for multicarrier modulation, should exhibit the desired orthogonality. Further, the real and imaginary parts of the complex bases should be spectrally similar and also orthogonal to each other. One such design method based on combined sine and cosine modulation has been described in [4]. However, the design contains too many constraints resulting in poorer stopband attenuation. In this paper, we first present two methods of designing complex multicarrier bases using cosine modulated filter bank. The motivation for using the cosine modulated filter bank is that there exists fast algorithm such as fast DCT [1] for implementing the filter bank. Next, we compare the performance of the wavelet packet based modulation scheme with that of discrete multitone modulation using DFT bases.

2. METHODS OF DESIGNING COMPLEX BASES

Before discussing the methods, we introduce the notation: Bold faced upper and lower case letters denote matrices and vectors, respectively. $\mathbf{B}^T$, $\mathbf{B}^*$ and $\mathbf{B}^\dagger$ represent transpose, conjugate and conjugate-transpose of $\mathbf{B}$. $\tilde{\mathbf{H}}(z) = \mathbf{H}^\dagger(1/z^*)$, $\mathbf{I}$ is the identity matrix, $\delta(n)$ is the unit impulse function, $x(n) * y(n)$ denotes convolution of $x(n)$ and $y(n)$, $F(z)$ is z-transform of $f(n)$ and E is the expectation operator.

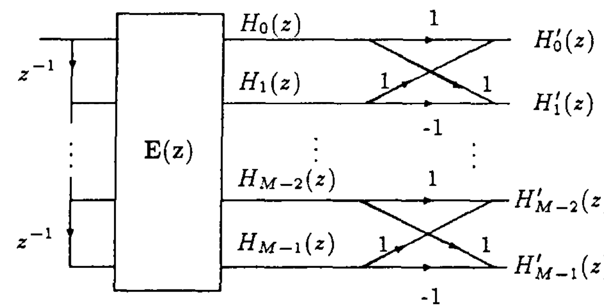

Figure 1: M-band modified cosine modulated filter bank

2.1 Method 1

We first design an M-band (M even) cosine modulated filter bank [1,3] $\mathbf{h}^T(z) = [H_0(z)\ H_1(z)\ \cdots\ H_{M-1}(z)]$. Let $\mathbf{E}(z)$ denote the polyphase matrix of the filter bank. Then $\mathbf{h}(z) = \mathbf{E}(z)\mathbf{e}(z)$ where $\mathbf{e}^T(z) = [1\ z^{-1} \cdots z^{-M+1}]$. The orthogonality of the bases (i.e., the impulse responses) corresponding to the cosine modulated filter bank follow from the fact that $\mathbf{E}(z)$ is paraunitary.

To get a pair of bases in the same band, we generate a modified filter bank $\mathbf{h}'^T(z) = [H_0'(z)\ H_1'(z)\ \cdots\ H_{M-1}'(z)]$ as shown in Fig. 1. The modified filter bank can be represented as

$$\mathbf{h}'(z) = \mathbf{R}\mathbf{h}(z) = \mathbf{R}\mathbf{E}(z)\mathbf{e}(z) \tag{1}$$

where

$$\mathbf{R} = \begin{bmatrix} 1 & 1 & 0 & 0 & \cdots & 0 \\ 1 & -1 & 0 & 0 & \cdots & 0 \\ 0 & 0 & 1 & 1 & \cdots & 0 \\ 0 & 0 & 1 & -1 & \cdots & 0 \\ . & . & . & . & \cdots & . \end{bmatrix} \tag{2}$$

The polyphase matrix of the new filter bank, $\mathbf{E}'(z)$, is $RE(z)$. Since $\mathbf{R}^T\mathbf{R} = 2\mathbf{I}$, we have

$$\tilde{\mathbf{E}}'(z)\mathbf{E}'(z) = \tilde{\mathbf{E}}(z)\mathbf{R}^T\mathbf{R}\mathbf{E}(z) = \tilde{\mathbf{E}}(z)2\mathbf{I}\mathbf{E}(z) = 2\mathbf{I} \tag{3}$$

Thus, $\mathbf{E}'(z)$ is paraunitary, which implies that the bases corresponding to the modified filter bank satisfy the orthogonality relation

$$\sum_n h'_k(n) h'_l(n+rM) = 2\delta(k-l)\delta(r), \; 0 \leq k, l \leq M-1 \quad (4)$$

where r is an integer. The bandwidth of the modified filters is twice that of the original cosine modulated filters. They are spectrally similar in pairs, at least in the passband. The spectral similarity of a pair, for 2 pairs of filters, is shown in Fig. 2. From the filters so generated, we form complex bases with the pair of bases corresponding to the filters in the same band as the real and imaginary parts. We thus obtain $M/2$ complex bases from M-band cosine modulated filter bank.. Now, to get real output from the complex multicarrier modulator, we require a second set of $M/2$ complex bases that are conjugates of the $M/2$ bases obtained as above. The M complex bases are:

$$\begin{aligned} f_k(n) &= h'_{2k}(n) + jh'_{2k+1}(n) & (5) \\ f_{M-1-k}(n) &= h'_{2k}(n) - jh'_{2k+1}(n) & (6) \end{aligned}$$

for $0 \leq k \leq M/2 - 1$ and $0 \leq n \leq L$ where L is the length of the prototype filter.

2.2 Method 2

In this method, we first design an $M/2$-band cosine modulated filter bank. We know that the impulse responses of these filters are orthogonal to their $rM/2$ shifted versions. Let the bases corresponding to this bank be denoted by $h''_k(n)$, $0 \leq k \leq M/2 - 1$. Then, we form the complex bases as follows:

$$\begin{aligned} f_k(n) &= h''_k(n) + jh''_k(n - M/2) & (7) \\ f_{M-1-k}(n) &= h''_k(n) - jh''_k(n - M/2) & (8) \end{aligned}$$

for $0 \leq k \leq M/2 - 1$ and $0 \leq n \leq L_1 + M/2 - 1$ where L_1 is the length of the prototype filter. It is now evident that the real and imaginary parts of these complex bases are spectrally identical and orthogonal.

2.3 Comparison of Different Bases

The amplitude responses of the Fourier transform of the real and imaginary parts of the DFT bases differ significantly in both the passband and stopband. Also, the stopband attenuation is very poor, and hence, overlap of the subchannels is very high. On the other hand, in the case of wavelet packet bases, the amplitude responses corresponding to real and imaginary parts are almost same in the passband, and the attenuation in the stopband is much higher resulting in less overlap of the subchannels other than immediate neighbors. Note that the real and imaginary parts of the complex base, designed by Method 2, are spectrally identical. However, for the same prototype filter length as in Method 1, i.e., $L = L_1$, the stopband attenuation is less in Method 2 and also the length of the base in Method 2 is longer by $M/2$. The longer length means more computation.

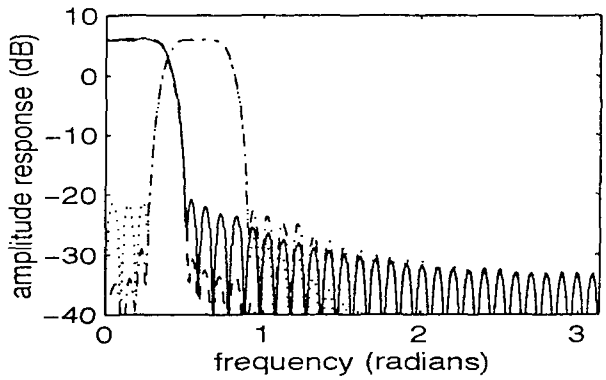

Figure 2: Frequency responses of the modified filters for $M = 16$ and $L = 64$ ($-H'_0(z)$, $--\ H'_1(z)$, $-\cdot-H'_2(z)$ and $\cdots H'_3(z)$).

3. MULTICARRIER SYSTEM

Consider the multicrrier system shown in Fig. 3. $\{s_m(t)\}$, $C(z)$ and $W(z)$ represent input complex symbols, channel and pre-detection equalizer, respectively. For the modulator output to be real, the input symbols should satisfy the relation $s_{M-m-1}(n) = s^*_m(n)$ for $0 \leq m \leq M/2 - 1$. $\{F_m(z)\}$ correspond to IDFT bases for the DMT case and complex wavelet packet bases given in (5) or (6) ((7) or (8)) for discrete wavelet multitone case. The m^{th} filter in the receiver is given by $F'_m(z) = z^{-d-gM}\tilde{F}_m(z)$. In the case of DMT $g = 1$, and in DWMT with Method 1 $gM = L$, while in DWMT with method 2 $gM = L_1$. Let $B'(z) = z^{-D}B(z)$ be the minimum mean square estimate of $C(z)W(z)$ [5] and p be the nominal delay introduced by the $B(z)$. Then, $d = KM - D - p$ (or $KM - D - p - M/2$ for Method 2) where K is chosen to make d non-negative.

For a simple delay channel with a delay of $p + D$, the input symbol for m^{th} subchannel in l^{th} block and the corresponding m^{th} subchannel output at the receiver are related as $s_m(l) = \theta_m(l + g_1)$ where $g_1 = g + K$.

For an arbitrary channel, the carriers at the input of the receiver will not be orthogonal, and there will be inter symbol interference (ISI) both across the subchannels and also across the blocks. To mitigate the effect of ISI, we use a post-detection equalizer [2] which combines the receiver output samples to give

$$\hat{s}_{m_1}(i_1) = \sum_{k=-\nu}^{\nu} \sum_{m' \in \Omega(m_1)} \lambda_{m_1}(m', k)\theta_{m'}(i_1 + k + g_1) \quad (9)$$

Here $\hat{s}_{m_1}(i_1)$ is an estimate of $s_{m_1}(i_1)$, $\Omega(m_1)$ denotes the set of indices of the subchannels that are involved in the estimation of the symbols in the m_1^{th} subchannel and ν denotes the number of blocks prior to and after the desired block. The design of the equalizer is equivalent to choosing the parameters $\lambda_{m_1}(m', k)$. As we see later, the performance of the equalizer depends on the number of subchannels used in the equalization.

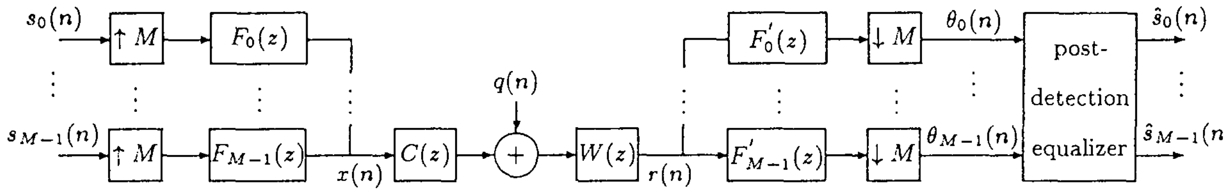

Figure 3: Discrete multicarrier modulation system

From Fig. 3, the transmitter and pre-detection equalizer outputs are

$$x(n) = \sum_{m=0}^{M-1}\sum_{l} s_m(l) f_m(n-lM) \tag{10}$$

$$r(n) = w(n) * c(n) * x(n) + w(n) * q(n) \tag{11}$$

where {q(n)} is the channel noise sequence. The output of m_1^{th} subchannel of the receiver is then given by

$$\begin{aligned}\theta_{m_1}(n) &= \sum_i r(i) f'_{m_1}(Mn-i)\\ &= \sum_{m=0}^{M-1}\sum_{l} s_m(l) h_{m,m_1}(M(n-l))\\ &\quad + \sum_i q(i)\bar{f}_{m_1}(Mn-i)\end{aligned} \tag{12}$$

where

$$h_{m,m_1}(n) = f_m(n) * c(n) * w(n) * f'_{m_1}(n) \tag{13}$$

$$\simeq f_m(n) * b'(n) * f'_{m_1}(n) \tag{14}$$

and

$$\bar{f}_m(n) = w(n) * f'_m(n) \tag{15}$$

Following the steps as in [2], we determine the coefficients of the post-detection equalizer, $\lambda_{m_1}(m',k)$. The estimate of $s_{m_1}(i_1)$ is given by

$$\begin{aligned}\hat{s}_{m_1}(i_1) =&\\ &\sum_{k=-\nu}^{\nu}\sum_{m'} \lambda_{m_1}(m',k) s_{m_1}(i_1) h_{m_1,m'}((k+g_1)M)\\ &+ \sum_{k=-\nu}^{\nu}\sum_{m'} \lambda_{m_1}(m',k) \sum_{m,l}{}' s_m(l)\\ &\quad .h_{m,m'}((k+g_1+i_1-l)M)\\ &+ \sum_{k=-\nu}^{\nu}\sum_{m'} \lambda_{m_1}(m',k) \sum_i q(i)\bar{f}_{m'}((k+g_1+i_1)M-i)\\ =&\ a_{m_1}(i_1)s_{m_1}(i_1) + \sum_{m,l}{}' a_m(l)s_m(l) + z_{m_1}(i_1)\end{aligned} \tag{16}$$

The primed sum denotes sum over all pairs $(m,l) \neq (m_1,i_1)$, $a_m(l) = \mathbf{v}_{m_1}^T \mathbf{a}_{l,m}$ and $z_{m_1}(i_1) = \mathbf{v}_{m_1}^T \mathbf{q}_{i_1,m_1}$. Vector $\mathbf{v}_{m_1}$ is obtained by stacking $\lambda_{m_1}(m',k)$, $k = -\nu,\cdots,\nu$, $m' \in \Omega(m_1)$. The t^{th} element of vector $\mathbf{a}_{l,m}$ is

$$\mathbf{a}_{l,m}(t) = h_{m,m(t)}((i_1+k(t)+g_1-l)M) \tag{17}$$

where $m(t)$ and $k(t)$ denote the indices m' and k, respectively, of the t^{th} element of $\mathbf{v}_{m_1}$. The t^{th} element of vector $\mathbf{q}_{i_1,m_1}$ is

$$\mathbf{q}_{i_1,m_1}(t) = \sum_i \bar{f}_{m(t)}((i_1+k(t)+g_1)M-i)q(i) \tag{18}$$

Now $E[|z_{m_1}(i_1)|^2] = \mathbf{v}_{m_1}^\dagger \mathbf{C}\mathbf{v}_{m_1}$, where $\mathbf{C} = E[\mathbf{q}_{i_1,m_1}^* \mathbf{q}_{i_1,m_1}^T]$. The elements of $\mathbf{C}$ are given by

$$\begin{aligned}\mathbf{C}(t_1,t_2) &= \sum_i\sum_l \bar{f}^*_{m(t_1)}((i_1+g_1+k(t_1))M-i)\\ &\quad .\bar{f}_{m(t_2)}((i_1+g_1+k(t_2))M-l)\psi(i-l)\end{aligned}$$

where $\psi(n)$ is the auto-correlation function of $q(n)$.

We now maximize the signal to interference plus noise ratio, given by

$$\begin{aligned}\gamma_{m_1}(i_1) &= \frac{|a_{m_1}(i_1)|^2}{E[|z_{m_1}(i_1)|^2] + \sum'_{l,m}|a_m(l)|^2}\\ &= \frac{\mathbf{v}_{m_1}^\dagger \mathbf{a}_{i_1,m_1}^* \mathbf{a}_{i_1,m_1}^T \mathbf{v}_{m_1}}{\mathbf{v}_{m_1}^\dagger \mathbf{B}\mathbf{v}_{m_1}}\end{aligned} \tag{19}$$

where $\mathbf{B} = \mathbf{C} + \sum'_{l,m}\mathbf{a}_{l,m}^*\mathbf{a}_{l,m}^T$. $\mathbf{B}$ is conjugate symmetric and we assume it to be nonsingular. Let $\mathbf{u} = \mathbf{B}^{*-1/2}\mathbf{a}_{i_1,m_1}$. Then

$$\gamma_{m_1}(i_1) = \frac{(\mathbf{u}^T\mathbf{B}^{1/2}\mathbf{v}_{m_1})^\dagger(\mathbf{u}^T\mathbf{B}^{1/2}\mathbf{v}_{m_1})}{(\mathbf{B}^{1/2}\mathbf{v}_{m_1})^\dagger(\mathbf{B}^{1/2}\mathbf{v}_{m_1})} \tag{20}$$

From Schwartz inequality, $\gamma_{m_1}(i_1)$ is maximum and equal to $\mathbf{u}^T\mathbf{u}$ when $\mathbf{u} \propto (\mathbf{B}^{1/2}\mathbf{v})^*$. With normalization of $a_{m_1}(i_1) = 1$, we obtain the vector $\mathbf{v}_{m_1}$ as

$$\mathbf{v}_{m_1} = \frac{\mathbf{B}^{-1}\mathbf{a}_{i_1,m_1}^*}{\mathbf{a}_{i_1,m_1}^\dagger \mathbf{B}^{-1*}\mathbf{a}_{i_1,m_1}} \tag{21}$$

This is determined for $m_1 = 0,\cdots,M/2-1$.

TABLE 1. Number of bits in error per 6000 bits in each subchannel for the DWMT system with complex bases of Method 1 for 16-QAM constellation

$\lvert\Omega(m_1)\rvert$		subchannel number								average bit error probability
		0	1	2	3	4	5	6	7	
6	no noise	172	0	0	0	64	247	854	687	0.04217
	30 dB SNR	188	0	0	0	93	271	895	709	0.04492
10	no noise	165	0	0	0	58	246	847	684	0.04167
	30 dB SNR	193	0	0	0	85	267	892	704	0.04460

TABLE 2. Number of bits in error per 3000 bits in subchannels 0 & 8 and per 6000 bits in other subchannels for the DMT system for 16-QAM constellation

$\lvert\Omega(m_1)\rvert$		subchannel number									average bit error probability
		0	1	2	3	4	5	6	7	8	
6	no noise	703	7	17	90	146	317	493	889	353	0.06281
	30 dB SNR	686	10	19	97	164	328	499	876	367	0.06346
10	no noise	560	0	0	11	117	242	451	819	318	0.05246
	30 dB SNR	544	0	0	17	141	272	472	822	311	0.05373

4. SIMULATION RESULTS

We conducted simulations to compare the performance of the DWMT system with that of DMT. In both cases, we used $M = 16$ and 16-QAM signal constellation with uniform bit loading. We used the wavelet packet bases obtained from Method 1 with $L = 64$. The prototype filter was designed to minimize the stopband attenuation at the cost of a slight increase in the transition band. This results in significant overlap between the frequency responses of the adjacent bases only. The pre-detection equalizer $W(z)$, fixing its length at 5, and the channel target filter $B'(z)$ were designed following the procedure given in [5]. The channel $C(z)$ used in the simulation is taken from [6]. The impulse response of this filter is of length 14 and is given by [-.12 -.13 -.16 -.18 -.22 -.26 -.12 .68 .46 .26 .07 -.04 -.1 -.12]. We chose $\nu = 1$ in the DMT case and $\nu = 3$ for DWMT. To see the effect number of subchannels used in the equalization, we considered two cases with 6 and 10 (i.e., size of $\Omega(m_1)$, denoted by $|\Omega(m_1)|$, is chosen as 6 and 10), taking the bases and their conjugates in pairs. For example, for $m_1 = 2$ and $|\Omega(m_1)| = 6$, we used the pairs of bases corresponding to (1,14), (2,13) and (3,12) subchannels. Tables 1 and 2 give the number of detected bits in error for the two systems. We may point out here that the training bits, used for finding $W(z)$ and $B'(z)$, are not counted in the results.

We note the following from the results. The DWMT system gives significantly better performance than the DMT. Use of more subchannels in the equalization gives significant improvement in the case of DMT, while this improvement is marginal in the case of DWMT. This is because the overlap among the subchannels is high in the case of DMT. In fact, we have observed from the simulations that the performance of the DMT system using all the subchannels in the equalization is almost same as that of DWMT with $|\Omega(m_1)| = 6$.

Though for comparison purpose we have used same number of bits for all the subchannels, in practice, different number of bits will have to be used for different subchannels depending upon the channel response.

Other simulation results (not shown here) show that DWMT system using Method 2 bases yields slightly poorer performance compared to that with Method 1 bases, for both QAM and PM signals, because of slightly poorer stopband attenuation in the case of Method 2.

5. REFERENCES

[1] P.P.Vaidyanthan, *Multirate Systems and Filter Banks*, Englewood Cliffs, NJ: Prentice Hall, Inc., 1993.

[2] S.D.Sandberg and M.A.Tzannes, "Overlap Discrete Multitone Modulation for High Speed Copper Wire Communications", *IEEE J. Select. Areas Commun.*, vol. 13, no. 9, pp 1571-1585, Dec. 1995.

[3] R.D.Koilpillai and P.P.Vaidyanathan, "Cosine Modulated FIR Filter Banks Satisfying Perfect Reconstruction", *IEEE Trans. Signal Processing*, vol. 40, no. 4, pp 770-783, Apr. 1992.

[4] Yuan-Pei Lin and P.P.Vaidyanathan, "Linear Phase Cosine Modulated Maximally Decimted Filter Banks with Perfect Reconstruction", *IEEE Trans. Signal Processing*, vol. 42, no. 11, pp 2525-2539, Nov. 1995.

[5] J. S. Chow, *Finite Length Equalization for Multi-carrier Transmission Systems*, PhD Thesis, Stanford University, 1992.

[6] A. Ruiz et al, "Discrete Multiple Tone Modulation with Coset Coding for the Spectrally Shaped Channel", *IEEE Trans. Communications*, vol. 40, no. 6, pp 1012-1029, Jun. 1992.